

# White Dwarf Mass Distribution in the SDSS

S. O. Kepler<sup>1\*</sup>, S. J. Kleinman<sup>2</sup>, A. Nitta<sup>3</sup>, D. Koester<sup>4</sup>, B. G. Castanheira<sup>1</sup>,  
 O. Giovannini<sup>5</sup>, A. F. M. Costa<sup>1</sup>, and L. Althaus<sup>6</sup>

<sup>1</sup>*Instituto de Física, Universidade Federal do Rio Grande do Sul, 91501-900 Porto-Alegre, RS, Brazil*

<sup>2</sup>*Subaru Telescope, 650 N. A'Ohoku Place, Hilo Hawaii, 96720, USA*

<sup>3</sup>*Gemini Observatory, Hilo, Hawaii, 96720, USA*

<sup>4</sup>*Institut für Theoretische Physik und Astrophysik, Universität Kiel, 24098 Kiel, Germany*

<sup>5</sup>*Universidade de Caxias do Sul, 95070-560 Caxias do Sul, RS, Brazil*

<sup>6</sup>*Facultad de Ciencias Astronómicas y Geofísicas, Paseo del Bosque S/N, (1900) La Plata - Argentina*

Accepted 2006 December 6. Received 2006 November 22; in original form 2006 August 1

## ABSTRACT

We determined masses for the 7167 DA and 507 DB white dwarf stars classified as single and non-magnetic in data release four of the Sloan Digital Sky Survey (SDSS). We obtained revised  $T_{\text{eff}}$  and  $\log g$  determinations for the most massive stars by fitting the SDSS optical spectra with a synthetic spectra grid derived from model atmospheres extending to  $\log g = 10.0$ . We also calculate radii from evolutionary models and create volume-corrected mass distributions for our DA and DB samples. The mean mass for the DA stars brighter than  $g=19$  and hotter than  $T_{\text{eff}} = 12\,000$  K is  $\langle M \rangle_{\text{DA}} \simeq 0.593 \pm 0.016 M_{\odot}$ . For the 150 DBs brighter than  $g=19$  and hotter than  $T_{\text{eff}} = 16\,000$  K, we find  $\langle M \rangle_{\text{DB}} = 0.711 \pm 0.009 M_{\odot}$ . It appears the mean mass for DB white dwarf stars may be significantly larger than that for DAs. We also report the highest mass white dwarf stars ever found, up to  $1.33 M_{\odot}$ .

**Key words:** stars – white dwarf

## 1 INTRODUCTION

White dwarf stars are the end product of evolution of all stars with initial masses up to around  $9 M_{\odot}$  and their distribution contains information about star formation history and

\* kepler@if.ufrgs.br

subsequent evolution in our Galaxy. As the most common endpoints of stellar evolution, white dwarf stars account for around 97% of all evolved stars. Considering there has not yet been enough time for any of them to cool down to undetectability, they can also provide independent information about the age of the Galaxy. Through an initial–final mass relation (IFMR), we can also study mass loss throughout the stellar evolution process. Because white dwarf progenitors lose carbon, nitrogen, and oxygen at the top of the asymptotic giant branch, they are significant contributors to the chemical evolution of the Galaxy and possibly an important source of life sustaining chemicals.

Kleinman et al. (2004) published the spectra of 2551 white dwarf stars in the Sloan Digital Sky Survey (SDSS) Data Release 1 (DR1), covering  $1360 \text{ deg}^2$ . Eisenstein et al. (2006) extended the white dwarf spectroscopic identifications to the 4th SDSS Data Release with a total of 9316 white dwarf stars reported, more than doubling the number of spectroscopically identified stars (McCook & Sion 2003). In both works, the authors fit the entire optical spectra from  $3900\text{\AA}$  to  $6800\text{\AA}$  to DA and DB grids of synthetic spectra derived from model atmospheres calculated by Detlev Koester, up to  $\log g = 9.0$ . Their fits include SDSS imaging photometry and allow for refluxing of the models by a low-order polynomial to incorporate effects of unknown reddening and spectrophotometric errors. The SDSS spectra have a mean g-band signal-to-noise ratio  $\text{SNR}(g) \approx 13$  for all DAs, and  $\text{SNR}(g) \approx 21$  for those brighter than  $g=19$ .

This large sample of stars with spectroscopic fits gives us a new opportunity to fully explore the white dwarf mass distribution. Understanding the white dwarf mass distribution offers insights into mass loss during stellar evolution, the IFMR, and has bearings on close binary star evolution. Our report, as well as many previous studies, detect a substantial fraction of low mass white dwarf stars that theoretically cannot have evolved as single stars, because the age of the Universe is smaller than their presumed lifetimes on the main sequence.

Kleinman et al. (2004) notice an increase in mean  $\log g$  for stars cooler than  $T_{\text{eff}} = 12000 \text{ K}$ , but caution the trend might not be real, indicating a problem in the data or fit technique, instead. The trend has persisted into the larger catalog of Eisenstein et al. (2006). Madej, Nalezyty, & Althaus (2004) analyzed the Kleinman et al. (2004) sample of fits and calculated the corresponding SDSS DR1 pure hydrogen atmosphere (DA) white dwarf mass distribution. As expected from the  $\log g$  trend, they found that the mean mass also increased below  $T_{\text{eff}} = 12000 \text{ K}$ . Their Table 1 presents all previous mean mass determinations, pro-

ducing an average of  $0.57 M_{\odot}$ , and a most populated peak at  $0.562 M_{\odot}$  for the 1175 stars hotter than  $T_{\text{eff}} = 12000$  K. They did not study the potentially highest mass stars with  $\log g > 9$ , because they were limited by the stellar atmosphere fit by Kleinman et al. (2004) which artificially pegged stars near the upper  $\log g = 9.0$  boundary to the boundary itself.

The increase in mean masses fitted from optical spectra below  $T_{\text{eff}} = 12000$  K has been seen prior to Kleinman et al. (2004) and has been discussed since Bergeron, Wesemael, & Fontaine (1991) and Koester (1991). It is usually dismissed as due to problems in the models: either convection bringing up subsurface He to the atmosphere, increasing the local pressure, or problems with the treatment of the hydrogen level occupation probability. The new larger SDSS data set, however, now gives another opportunity to explore this trend and evaluate its cause.

Most reported white dwarf mass determinations have been derived by comparing the optical spectra with model atmospheres, as with Kleinman et al. (2004) and Eisenstein et al. (2006). For the DA stars, the H7, H8 and H9 lines, in the violet, are the most sensitive to surface gravity because they are produced by electrons at higher energy levels, those most affected by neighboring atoms. However, these lines are also in the region where the atmospheric extinction is the largest and typical CCD detectors are the least sensitive. As a consequence, most studies used only the line profiles in their fits, avoiding the dependence on often uncertain flux calibrations. The SDSS white dwarf spectra have good flux calibration and acceptable SNR redwards of 4000Å. The published SDSS catalog therefore fits the *entire* optical spectrum, and not just the H lines, as has been traditionally done. The rationale for this approach is the good, uniform spectrophotometry and corresponding broad band photometry that can be used in the fits. In addition, a low-level re-fluxing is allowed to take out large errors in spectrophotometry and any unknown reddening effects.

In this paper, we will compare the measured white dwarf mass distributions from Kleinman et al. (2004) and Eisenstein et al. (2006) with previous determinations and attempt to assess the reason for the observed increase in mass for lower temperatures. We will also explore the observed mean masses and analyze the two different fitting techniques: line profile vs. whole spectrum, to see the effects on the resulting mass distributions.

## 2 DATA AND MODELS

The SDSS imaged the high Galactic latitude sky in five passbands: u, g, r, i and z, and obtained spectra from 3800Å to 9200Å with a resolution of  $\approx 1800$  using a twin fiber-fed spectrograph (York et al. 2000). Since we are primarily interested in the mass distribution here, we selected only the single DA and DB stars with  $\log g - \sigma_{\log g} \geq 8.5$  and  $\log g + \sigma_{\log g} \leq 6.5$  from the Eisenstein et al. (2006) sample and refit them with an expanded grid of models (see below), using the same *autofit* routine as in Eisenstein et al. (2006) and thoroughly described in Kleinman et al. (2004). We excluded all stars classified by Eisenstein et al. (2006) as having either a detectable magnetic field or a companion, metal lines, DABs, and DBAs.

Our model grid (Finley, Koester, & Basri 1997; Koester et al. 2001) is similar to that used by Eisenstein et al. (2006), but extended in  $T_{\text{eff}}$  and  $\log g$  ( $100\,000 \text{ K} \leq T_{\text{eff}} \leq 6000 \text{ K}$ ,  $10.0 \leq \log g \leq 5.0$ ) and denser. We chose the  $\text{ML2}/\alpha = 0.6$  parameterization for convection as demonstrated by Bergeron et al. (1995) to give internal consistency between temperatures derived in the optical and the ultraviolet, photometry, parallax, and with gravitational redshift. ML2 corresponds to the Bohm & Cassinelli (1971) description of the mixing length theory and  $\alpha = \ell/\lambda_P$  is the ratio of the mixing length to the pressure scale height. The models include the  $H_2^+$  and  $H_2$  quasi-molecular opacities and only Stark (Lemke 1997) and Doppler broadening, so the line profiles are not precise for  $T_{\text{eff}} < 8500 \text{ K}$ .

Even though Napiwotzki, Green, & Saffer (1999) and Liebert, Bergeron, & Holberg (2005) discuss the necessity of using NLTE atmospheres for the stars hotter than 40 000 K, all quoted values are from LTE models, as they also show the NLTE corrections are not dominant, and our number of hot stars is small.

To calculate the mass of each star from the  $T_{\text{eff}}$  and  $\log g$  values obtained from our fits, we used the evolutionary models of Wood (1995) and Althaus et al. (2005) with C/O cores up to  $\log g = 9.0$ , and O/Ne cores for higher gravities,  $M_{\text{He}} = 10^{-2} M_*$ , and  $M_{\text{H}} = 10^{-4} M_*$ , or  $M_{\text{H}} = 0$ , to estimate stellar radii for DAs and DBs, respectively. The radius is necessary to convert surface gravity to mass.

## 3 ANALYSIS

Before exploring the mass distributions, we wanted to examine the different fitting techniques used in the available data sets — the traditional line profile technique and the SDSS whole

spectrum approach. We therefore simulated spectra with differing SNRs by adding random noise to our models and fit them with our own set of both line profile and whole spectrum fitting routines. Our Monte Carlo simulations show that in the low SNR regime,  $\text{SNR} \leq 50$ , fitting the whole spectra and not just the line profiles gives *more* accurate atmospheric parameters, as long as the flux calibration or interstellar reddening uncertainties do not dominate. We estimate an uncertainty of around  $\Delta T_{\text{eff}} \simeq 500$  K and  $\Delta \log g \simeq 0.10$  at  $\text{SNR}=40$  for the whole spectra fitting. For  $\text{SNR}=20$ , similar to the average SDSS spectra for  $g < 19$ , our simulations indicate  $\Delta T_{\text{eff}} \simeq 750$  K and  $\Delta \log g \simeq 0.15$ . We do not report in this paper on the mass distribution for the stars fainter than  $g=19$  because their smaller SNR lead to large uncertainties. Our simulations did not indicate systematic trends between the two approaches.

Although Kleinman et al. (2004) and Eisenstein et al. (2006) compared their fits' internal errors by fitting duplicate spectra, they did not display their results as a function of temperature. Kepler et al. (2005) specifically analyzed 109 duplicate spectra SDSS DAs with  $13000 \text{ K} \geq T_{\text{eff}} \geq 10000 \text{ K}$ , near the region where the fit  $\log g$ s start to increase. They showed that the mean fit differences were  $\sigma_{T_{\text{eff}}} \simeq 300$  K and  $\sigma_{\log g} \simeq 0.21$  dex for the same object but different observations. These values are larger than the internal uncertainty of the fits, but in general within  $3\sigma$  of each other, as in Kleinman et al. (2004) and Eisenstein et al. (2006). We thus conclude that the uncertainties in Eisenstein et al. (2006) are reasonable and can now analyze the results without attributing any noted irregularities to the fitting process.

Kepler et al. (2006), however, compare SDSS spectra with new  $\text{SNR}(g) \simeq 100$  spectra acquired with GMOS on the Gemini 8 m telescope for four white dwarf stars around  $T_{\text{eff}} \simeq 12\,000$  K. Their fits suggest that published SDSS optical spectra fits overestimate the mass by  $\Delta \mathcal{M} \simeq 0.13 \mathcal{M}_{\odot}$ , because of the correlation between the derived  $T_{\text{eff}}$  and  $\log g$  — a small increase in  $T_{\text{eff}}$  can be compensated by a small decrease in  $\log g$ . Our simulations indicate this discrepancy is concentrated only in the region around the Balmer line maximum,  $14000 \text{ K} \geq T_{\text{eff}} \geq 11000 \text{ K}$ .

To explore the increasing mass trend in more detail, we restricted our sample to the 1733 stars both brighter than  $g=19$  and hotter than  $T_{\text{eff}} = 12\,000$  K and obtained an average DA mass of  $\langle \mathcal{M} \rangle_{\text{DA}} = 0.593 \pm 0.016 \mathcal{M}_{\odot}$ . The distribution for this hot and bright sample, shown in Fig. 1, is similar to that of the Palomar Green survey published by Liebert, Bergeron, & Holberg (2005). They studied a complete sample of 348 DA stars with

**Table 1.** Gaussian fits for the  $T_{\text{eff}} \geq 12\,000$  K and  $g \leq 19$  histogram, seen in Fig. 1.

i	$a_i$	$M_i(\mathcal{M}_\odot)$	$\sigma_i$	Fraction
1	264.8	0.578	0.047	69%
2	27.8	0.658	0.149	23%
3	27.0	0.381	0.050	7%
4	3.0	1.081	0.143	1%

SNR  $\geq 60$  spectra and determined atmospheric parameters by spectral fitting via the line profile fitting technique, using models up to  $\log g = 9.5$ . They found a peak in the mass histogram at  $0.565 \mathcal{M}_\odot$  containing 75% of the sample, a low mass peak with  $0.403 \mathcal{M}_\odot$  containing 10% of the sample, and a high mass peak at  $0.780 \mathcal{M}_\odot$  containing 15% of the stars. They fit their mass histogram (PG mass histogram from hereafter) with three Gaussian profiles:  $0.565 \mathcal{M}_\odot$  with  $\sigma \simeq 0.080 \mathcal{M}_\odot$ ,  $0.403 \mathcal{M}_\odot$  with  $\sigma \simeq 0.023 \mathcal{M}_\odot$ , and a broad high-mass component at  $0.780 \mathcal{M}_\odot$  with  $\sigma \simeq 0.108 \mathcal{M}_\odot$ . They found more stars above  $1 \mathcal{M}_\odot$  than can be described by the three Gaussians they fit. Vennes et al. (1997), Vennes (1999), and Marsh et al. (1997) also find an excess of white dwarf stars with masses above  $1 \mathcal{M}_\odot$  in their sample of  $T_{\text{eff}} > 23\,000$  K white dwarf stars.

The overall mass distribution of our bright sample matches well with that of the previous standard PG survey sample. We now explore the distribution with temperature.

In Fig. 2, we show the mass distribution vs. temperature for DA stars brighter than  $g = 19$  along with the similar distribution from Liebert, Bergeron, & Holberg (2005). Again, we see the distributions are roughly equivalent and we see an increase in measured mass at lower temperatures. Our histograms use  $0.025 \mathcal{M}_\odot$  bins ( $N/dm = \text{constant}$ ) because that is the approximately mean uncertainty in our mass determinations.

To explore the region of increasing mass further, Fig. 3 shows the mass histogram only for the 964 DAs brighter than  $g=19$ , and  $12\,000 \text{ K} \geq T_{\text{eff}} \geq 8\,500 \text{ K}$ , for which we obtain  $\langle \mathcal{M} \rangle_{\text{DA}}^{\text{cool}} \simeq 0.789 \pm 0.005 \mathcal{M}_\odot$ . We have excluded the stars cooler than  $T_{\text{eff}} = 8500$  K from our mass histograms because our cooler atmospheric models are not accurate for  $\log g$  determination, as explained earlier.

Tables 1 and 2 detail the Gaussian fits we made for the histograms of Figures 1 and 3 respectively, with

$$N = \sum_i a_i \exp \left[ -\frac{(\mathcal{M} - \mathcal{M}_i)^2}{2\sigma_i^2} \right] \quad (1)$$

Figure 11 of Liebert, Bergeron, & Holberg (2005) also shows an increase in mass below  $T_{\text{eff}} = 12\,000$  K (see Fig. 2), even though they have a limited number of cooler stars due to

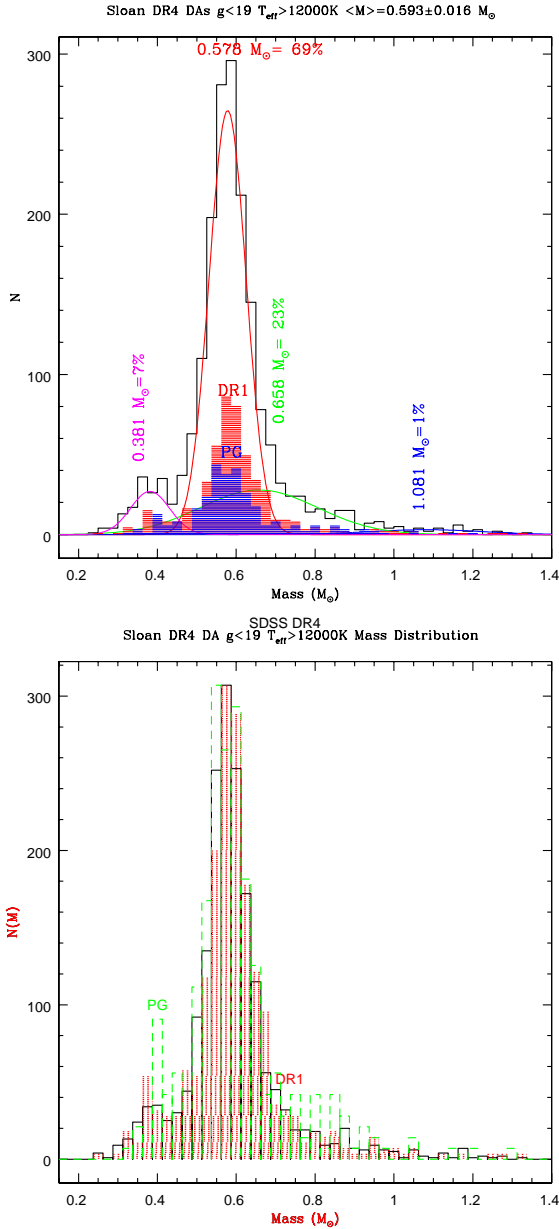


**Figure 1.** Histogram for the 1733 DA stars brighter than  $g=19$  and hotter than  $T_{\text{eff}} = 12\,000$  K, compared to the PG survey published by Liebert, Bergeron, & Holberg (2005) and the SDSS DR1 sample published by Madej, Nalezyty, & Althaus (2004). Gaussian fits detailed in Table 1 are also shown. Our bins are  $0.025 M_{\odot}$  wide. The second graph shows the DR1 and PG survey data normalized to the DR4 sample, even though those samples are smaller and therefore have significantly larger errorbars.

**Table 2.** Gaussian fits for the 964 DAs with  $12\,000 \text{ K} \geq T_{\text{eff}} \geq 8\,500 \text{ K}$  and  $g \leq 19$  histogram.

i	$a_i$	$M_i(M_{\odot})$	$\sigma_i$	Fraction
1	29.5	0.818	0.160	49%
2	59.6	0.793	0.052	33%
3	18.0	0.640	0.086	16%
4	13.4	1.096	0.136	2%

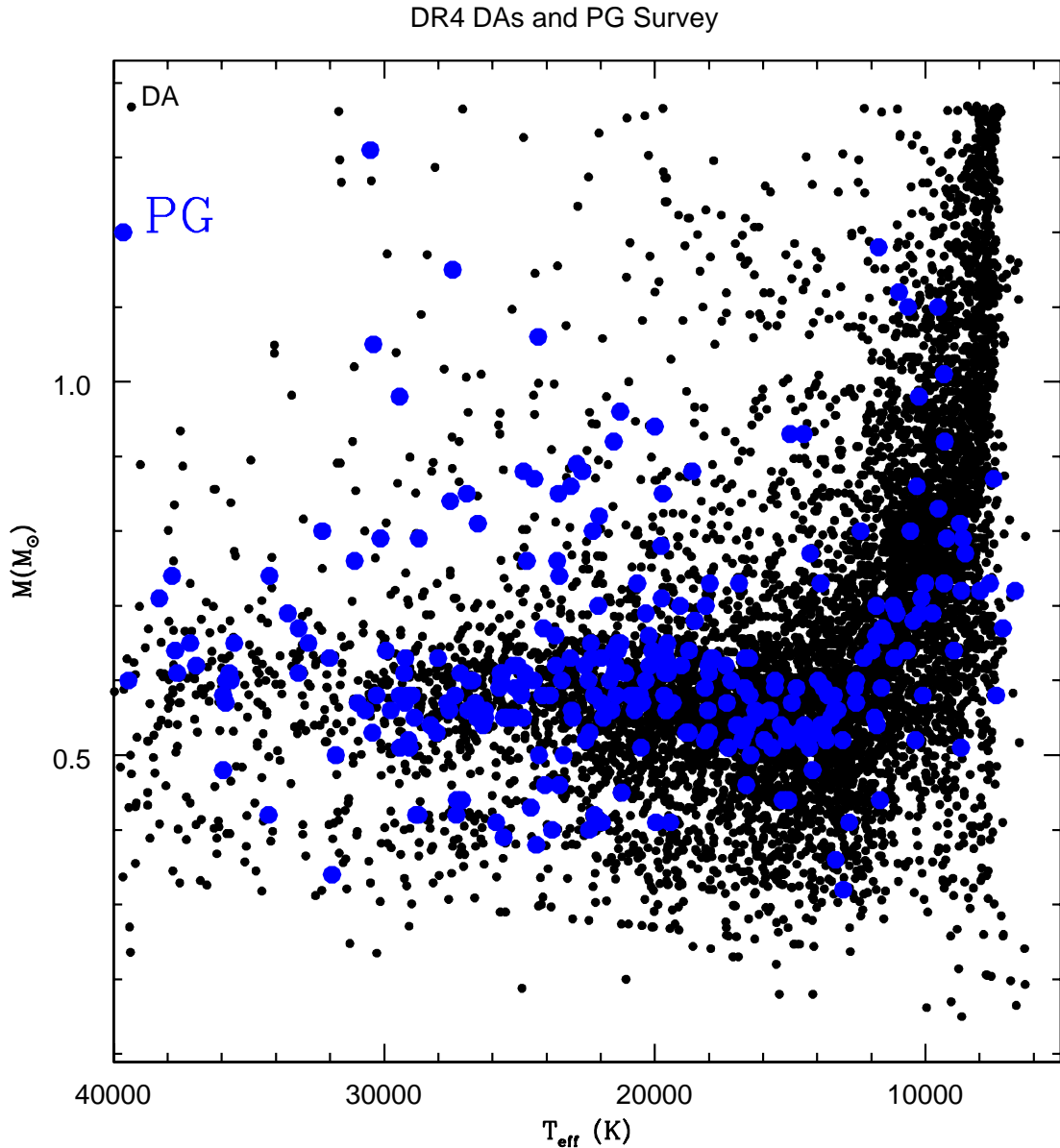


**Figure 2.** Masses for all 3595 DA white dwarf stars brighter than  $g=19$  and cooler than 40 000 K, showing an increase in mean mass for lower  $T_{\text{eff}}$ . The large solid (blue) circles are the values published by Liebert, Bergeron, & Holberg (2005), showing the increase in mass at lower  $T_{\text{eff}}$  is also present in their sample, which uses a totally independent grid of models and fitting technique.

color selection effects in the PG survey. It is important to note that the model atmospheres used in Liebert, Bergeron, & Holberg (2005) and the line profile fitting technique they use are totally independent of our own. Therefore, if the observed increase in the measured gravity with temperature is merely an artifact of the models, then similar problems must be present in two independent groups of models and fitting techniques. We are thus gathering increasing evidence that either a) both DAs and DBs really do have higher mean masses at

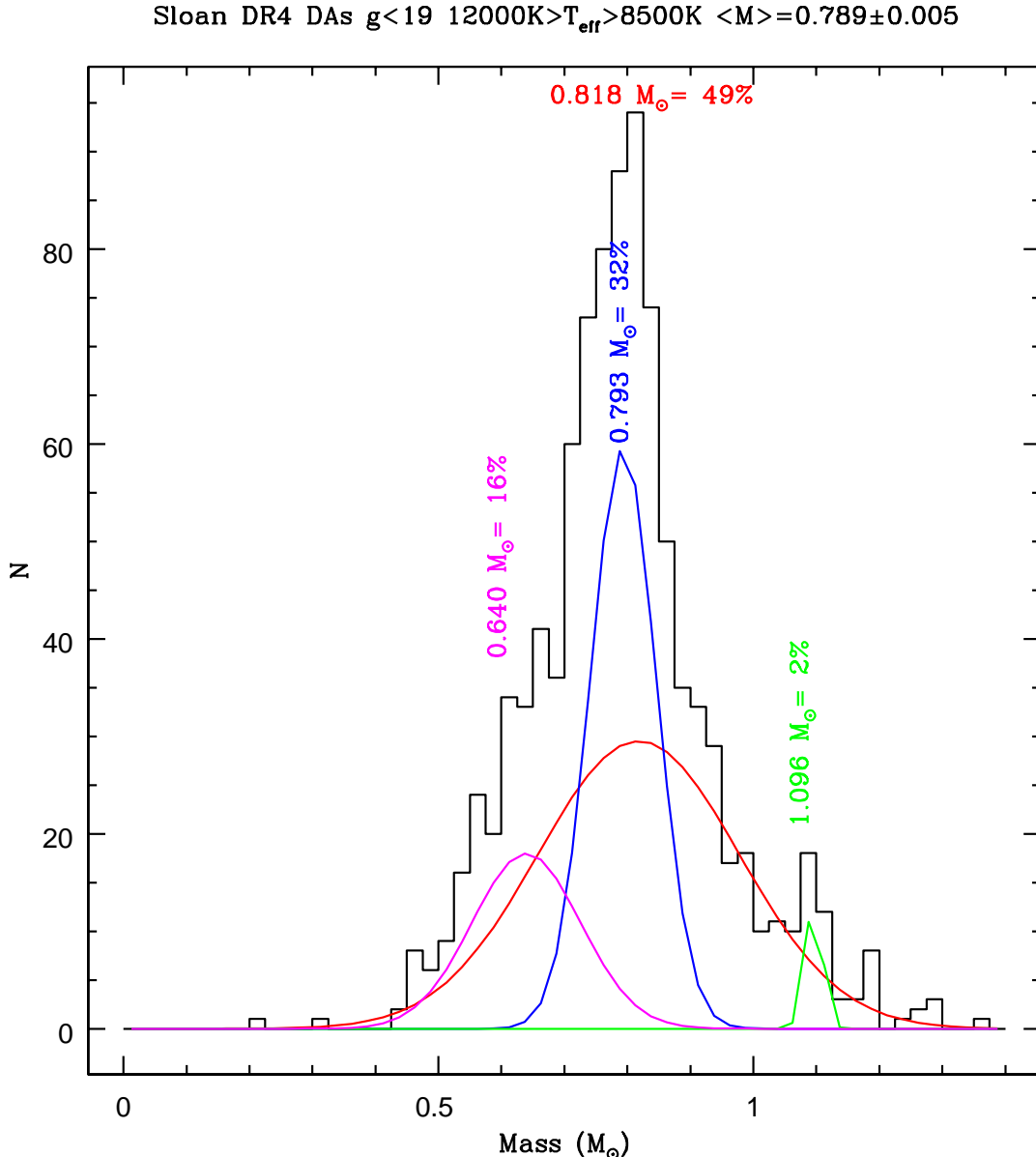


**Figure 3.** Histogram for the 964 DA stars brighter than  $g=19$ , with  $12000 \text{ K} \geq T_{\text{eff}} \geq 8500 \text{ K}$  along with the fit Gaussians as detailed in Table 2.

lower temperatures, or b) there is a common artifact in the model used for all white dwarf spectral fitting.

#### 4 WHY WE DO NOT TRUST MASSES FOR $T_{\text{EFF}} < 12000 \text{ K}$ FOR DA STARS

Bergeron et al. (1995) measured an increase in the mean mass for the ZZ Ceti star sample around  $13000 \text{ K} > T_{\text{eff}} > 11000 \text{ K}$ , but indicated it might come from a selection effect because the discovery of pulsating stars might have preferred higher mass stars. Arras, Townsley, & Bildsten

(2006), e.g., show that the white dwarf pulsators with lower masses should pulsate at cooler temperatures. Our sample of 351 bright stars in the same temperature range show a similar increase in mass compared to the hotter sample, but we have not been biased by the pulsators, so an observational bias is not the cause for the increase in mass detected.

The simple expectation that massive stars cool faster than their less massive counterparts does not hold for  $T_{\text{eff}} \leq 10\,000$  K, as the most massive stars have smaller radius and, therefore, their cooling slows down after a few e-folding timescales. Another possible explanation for an increased mean mass at lower effective temperatures is the presence of otherwise undetected He at the surface, broadening the observed H lines and thus mimicking a higher  $\log g$ . Theoretical models (e.g. Fontaine & Wesemael (1991)) indicate that only for DAs with hydrogen layer masses below  $\mathcal{M}_H = 10^{-10}\mathcal{M}_*$  will He mix around  $T_{\text{eff}} = 10\,000$  K and, if  $\mathcal{M}_H = 10^{-7}\mathcal{M}_*$ , only below  $T_{\text{eff}} \simeq 6\,500$  K. However, all seismologically measured H layer masses are  $\mathcal{M}_H > 10^{-7}\mathcal{M}_*$  (Bradley 2006, 2001, 1998; Fontaine & Wesemael 1997). Since our increased mass trend happens significantly hotter than  $T_{\text{eff}} = 6\,500$  K, He contamination cannot account for the observed increase in mass at lower temperatures, unless the more distant stars studied here have significantly thinner H layers. Lawlor and MacDonald's (2006) models show around 3% of the DAs could have  $\mathcal{M}_H \sim 10^{-9}\mathcal{M}_*$ , but not thinner. Therefore, there are not enough stars with thin H layers, at any rate, to account for our excess of massive objects.

Wilson (2000) proposes a possible physical model for increasing WD masses at lower temperatures. She suggests that low metallicity AGBs will produce higher mass white dwarf stars, probably around  $1\mathcal{M}_\odot$ , because the relatively lower mass loss expected for low metallicity AGB stars increases the mass of the core prior to the star moving out of the AGB. Since the earlier generations of white dwarf stars which have now cooled more than their later cohorts, presumably came from lower-metallicity progenitors, this mechanism could explain a mass increase at lower white dwarf temperatures. If we extend this concept to globular clusters though, we would expect the mass of the white dwarfs in globular clusters to be larger than the mean mass of our stars cooler than 10 000 K, which is not observed (Moehler et al. 2004; Richer et al. 2007). So again, we are left with a discarded explanation of the observed mass increase.

An interesting clue to the problem may be found in Engelbrecht & Koester (2007), which used SDSS photometry alone to make a mass estimate. Their cool white dwarf stars show mean masses similar to those of the hotter stars. Our mass determinations using photometric

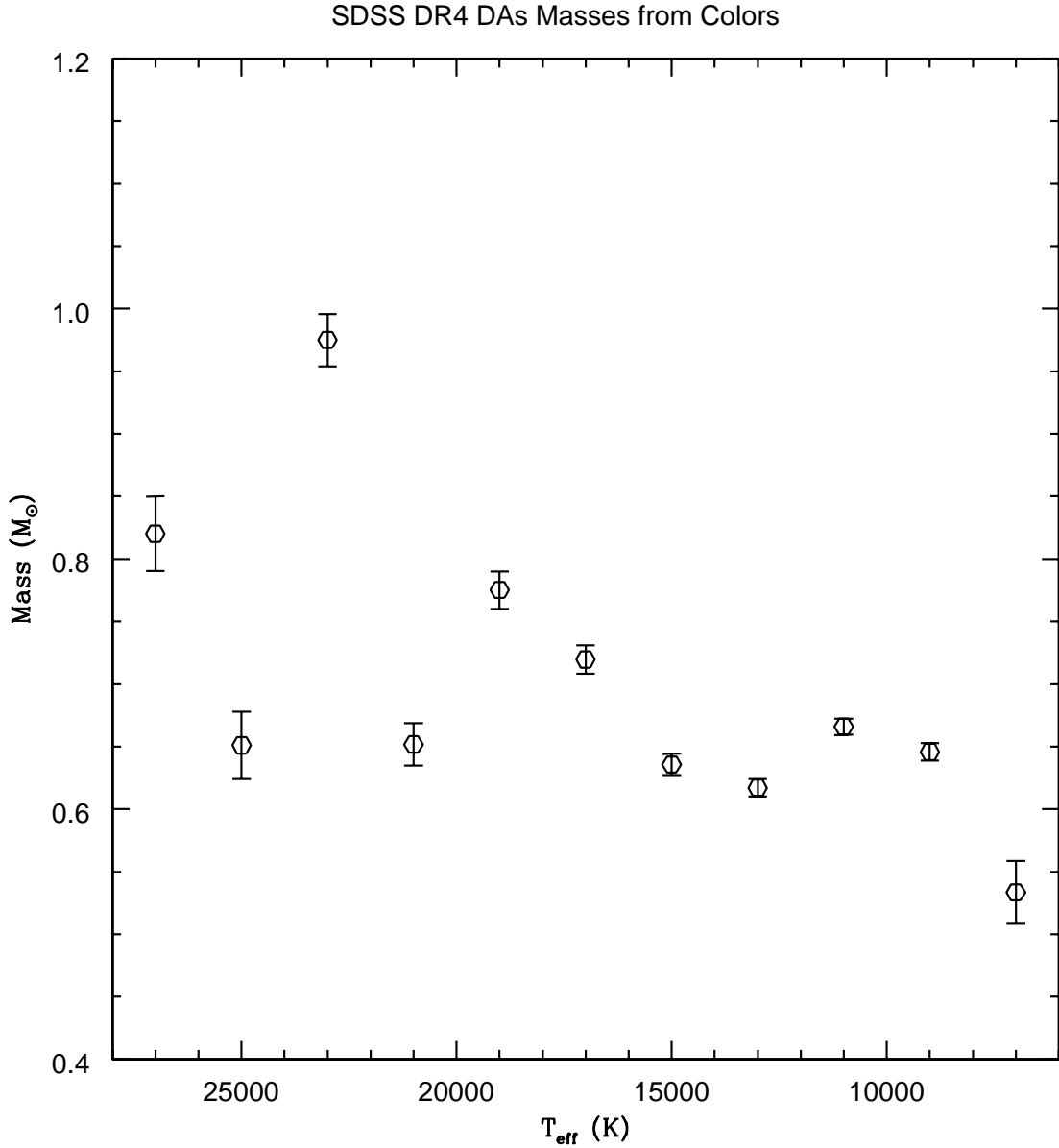


**Figure 4.** Masses for all 7167 DA white dwarf stars derived comparing only the SDSS colors (u-g) and (g-r) with those predicted from the atmospheric models. For  $T_{\text{eff}} \geq 20\,000\text{K}$  and  $T_{\text{eff}} \leq 9\,000\text{ K}$ , the colors are degenerate in mass.

colors only, shown in Fig. 4, is derived comparing only the SDSS colors (u-g) and (g-r) with those predicted from the atmospheric models convolved with SDSS filters. They do not show any increase in mass with decreasing  $T_{\text{eff}}$ . Because of their larger uncertainties than the spectra fitting, we binned the results in 2000 K bins. This result suggests that any problem in the models is mainly restricted to the line profiles, not the continua, which dominate the broadband photometric colors.

Thus, we are mainly left with the possibility raised by Koester (1991) that an increase in mass with lower temperatures could be due to the treatment of neutral particles in model

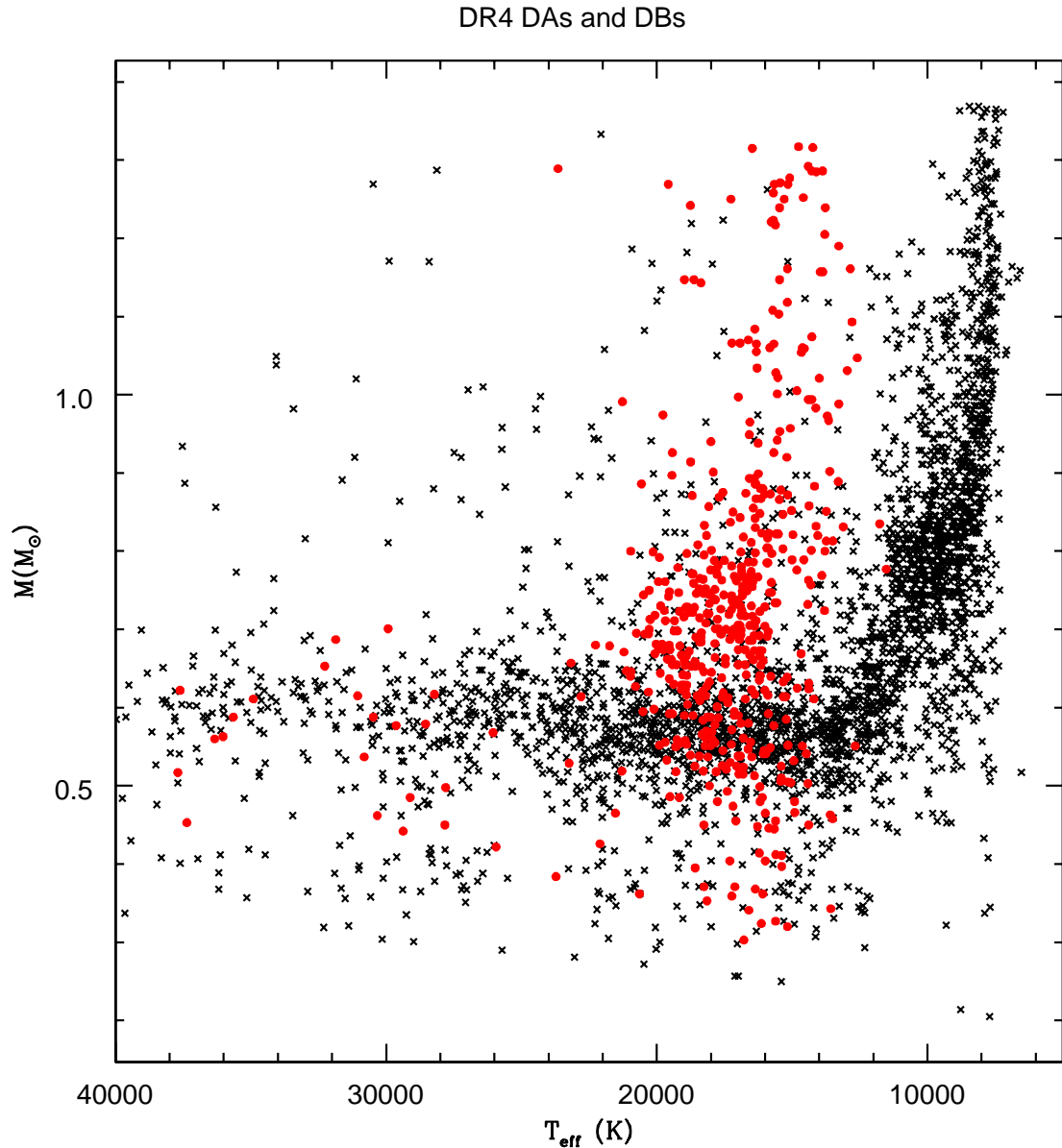


**Figure 5.** Masses for all 5718 DAs (crosses) cooler than 40 000 K and 507 DBs (filled circles) showing the continuous increase in average mass at lower  $T_{\text{eff}}$ .

atmospheres with the Hummer-Mihalas formalism. Bergeron et al. (1995), however, suggests that the neutral particles are only important below  $T_{\text{eff}} \simeq 8000$  K which is certainly lower than where we see the trend begin. It seems the only remaining explanation is that accurate modeling of neutral particles will indeed show an effect for DAs near 12 000 K.

## 5 DB WHITE DWARFS

We determined masses for the Eisenstein et al. (2006) DBs from their fit temperatures and gravities using evolutionary grids of Althaus et al. (2005); Althaus, Serenelli, & Benvenuto

**Table 3.** Gaussian fits for the histogram of the 150 DBs brighter than  $g=19$  and hotter than  $T_{\text{eff}} = 16\,000$  K.

i	$a_i$	$M_i(\mathcal{M}_\odot)$	$\sigma_i$	Fraction
1	8.3	0.700	0.109	59%
2	14.3	0.712	0.042	40%
3	0.6	1.288	0.035	1%

(2001). The Althaus models use time resolved diffusion throughout evolution. Metcalfe (2005) and Metcalfe et al. (2005a) discuss asteroseismological results in DBs, showing the observations are consistent with the layer masses predicted by current diffusion theory. Fig. 5 shows we find an increase in the measured surface gravity below  $T_{\text{eff}} \simeq 12\,000$  K for DAs and a similar increase below  $T_{\text{eff}} \simeq 16\,000$  K for DBs. For the 208 DBs brighter than  $g=19$ , we find  $\langle \mathcal{M} \rangle_{\text{DB}}^{\text{all}} = 0.785 \pm 0.013 \mathcal{M}_\odot$ . For the 150 DBs brighter than  $g=19$  and hotter than  $T_{\text{eff}} = 16\,000$  K, we find  $\langle \mathcal{M} \rangle_{\text{DB}} = 0.711 \pm 0.009 \mathcal{M}_\odot$ . Both measurements are considerably larger than the  $0.593 \mathcal{M}_\odot$  mean mass value for the bright and hot DA sample. A similar larger (relative to that of the DAs) DB mean mass value has been previously reported by Koester et al. (2001) who obtained a  $\langle \mathcal{M} \rangle_{\text{DB}} = 0.77$  for the 18 DBs they observed with UVES/VLT, including stars down to  $T_{\text{eff}} \sim 16\,000$  K. Others, however, find lower mean DB masses, more similar to those of the DAs. Oke, Weidemann, & Koester (1984) derived  $\langle \mathcal{M} \rangle_{\text{DB}} = 0.55 \pm 0.10$  from their sample of 25 DBs ranging  $30\,000 \text{ K} > T_{\text{eff}} > 12\,000$  K, while Beauchamp (1995) found  $\langle \mathcal{M} \rangle_{\text{DB}} = 0.59 \pm 0.01 \mathcal{M}_\odot$  for his 46 DBs, ranging  $12\,000 \text{ K} \geq T_{\text{eff}} \geq 31\,000$  K. For the 34 DBs in Castanheira et al. (2006), ranging  $27\,000 \text{ K} \geq T_{\text{eff}} \geq 13\,000$  K, the mean is  $\langle \mathcal{M} \rangle_{\text{DB}} = 0.544 \pm 0.05 \mathcal{M}_\odot$ .

The Gaussian fits for the 150 DBs brighter than  $g=19$  and hotter than  $T_{\text{eff}} = 16\,000$  K are listed in Table 3. The mass histogram for DBs is shown in Fig. 6.

## 6 OBSERVING VOLUME CORRECTION

In order to turn our observed mass distributions into a real analytical tool, we must first correct the sample for completeness. We do this by the  $1/V_{\text{max}}$  formalism.  $V_{\text{max}}$  is the volume defined by the maximum distance at which a given object would still appear in a magnitude limited sample (Schmidt 1968). Geijo et al. (2006) discuss white dwarf luminosity function completeness corrections and conclude that for large samples, the  $1/V_{\text{max}}$  method provides a reliable characterization of the white dwarf luminosity function.

Liebert, Bergeron, & Holberg (2005) find that 2.7% of the stars in the PG sample have masses larger than  $1 \mathcal{M}_\odot$  and, when corrected by  $1/V_{\text{max}}$ , 22% are above  $0.8 \mathcal{M}_\odot$ .

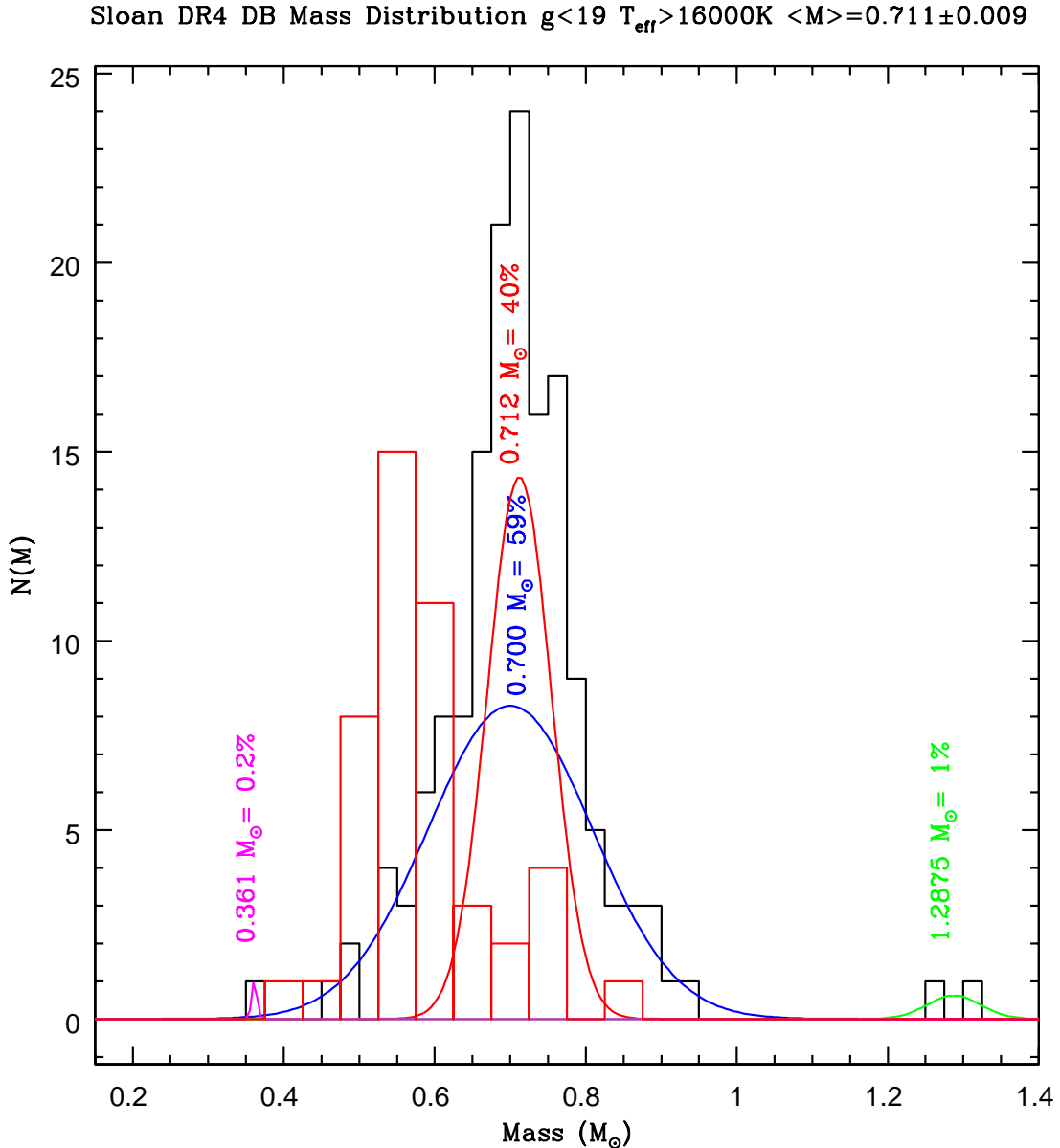


**Figure 6.** Histogram for the 150 DBs brighter than  $g=19$  and hotter than  $T_{\text{eff}} = 16000\text{ K}$  in DR4.

We first calculated each star's absolute magnitude from the  $T_{\text{eff}}$  and  $\log g$  values obtained from our fits (for the extreme mass ones) or those of Eisenstein et al. (2006) (for the rest), convolving the synthetic spectra with the g filter transmission curve. We used the evolutionary models of Wood (1995) and Althaus et al. (2005) with C/O cores up to  $\log g = 9.0$ , and O/Ne cores for higher gravities,  $M_{\text{He}} = 10^{-2} M_{\ast}$ , and  $M_{\text{H}} = 10^{-4}$  or  $0 M_{\ast}$ , to estimate stellar radii for DAs and DBs respectively. We do not claim that the SDSS spectroscopic sample is complete, but we do contend that in terms of mass, there should be no preferential bias in the target selection. Harris et al. (2006) report that spectra are obtained for essentially all

white dwarf stars hotter than 22 000 K. Additional white dwarf stars down to  $T_{\text{eff}} = 8000$  K are also found, but few cooler than that as these stars overlap in color space with the F, G, and K main-sequence stars. Eisenstein et al. (2006) discuss the spectroscopic sample completeness, which is around 60% at  $18 < g < 19.5$  for stars hotter than  $T_{\text{eff}} = 12\,000$  K and around 40% for cooler stars. Our analysis is restricted to the sample brighter than  $g=19$ .

Once we had our calculated absolute magnitudes, we could estimate each star's distance as shown in Fig. 7, neglecting any effects of interstellar extinction. The mean distance for our DA samples are:  $474 \pm 5$  pc for the entire 7167 DA sample,  $302 \pm 5$  pc for the stars brighter than  $g=19$ , and  $436 \pm 7$  pc for the stars brighter than  $g=19$  and hotter than  $T_{\text{eff}} \simeq 12\,000$  K.

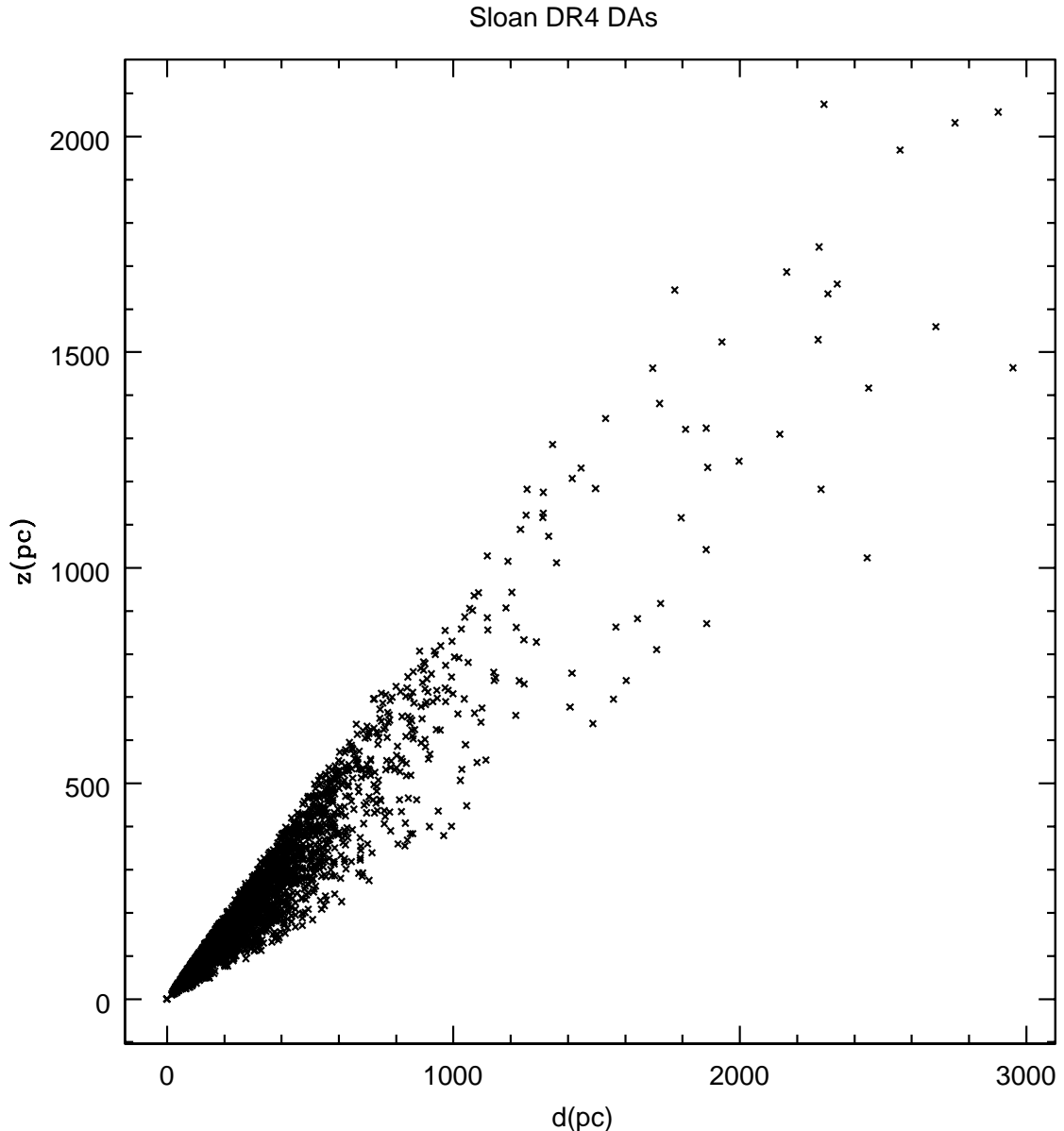
For each star in our sample, we calculate

$$V_{\text{max}} = \frac{4\pi}{3} \beta (r_{\text{max}}^3 - r_{\text{min}}^3) \exp(-z/z_0)$$

where  $\beta$  is the fraction of the sky covered, 0.1159 for the DR4 sample,  $r_{\text{min}}$  is due to the bright magnitude limit,  $g=15$ , and  $z_0$  is the disk scale height which we assume to be 250 pc, as Liebert, Bergeron, & Holberg (2005) and Harris et al. (2006), even though our height distribution indicates  $z_0 \simeq 310$  pc. Vennes et al. (2005) show that both the white dwarf stars in the SDSS DR1, and the 1934 DAs found in the 2dF ( $18.25 \leq b_J \leq 20.85$ ) quasar surveys, belong to the thin disk of our Galaxy. Using these data, they measured a scale height around 300 pc. Harris et al. (2006) calculate the white dwarf luminosity function from photometric measurements of the white dwarf stars discovered in the SDSS survey up to DR3. They assume  $\log g = 8.0$  for all stars and use the change in number per magnitude bin to calculate the scale height of the disk, obtaining  $340_{-70}^{+100}$  pc, but adopt 250 pc for better comparison with other studies. This volume includes the disk scale height as discussed by Green (1980); Fleming, Liebert, & Green (1986); and Liebert, Bergeron, & Holberg (2005). Each star contributes  $1/V_{\text{max}}$  to the local space density.

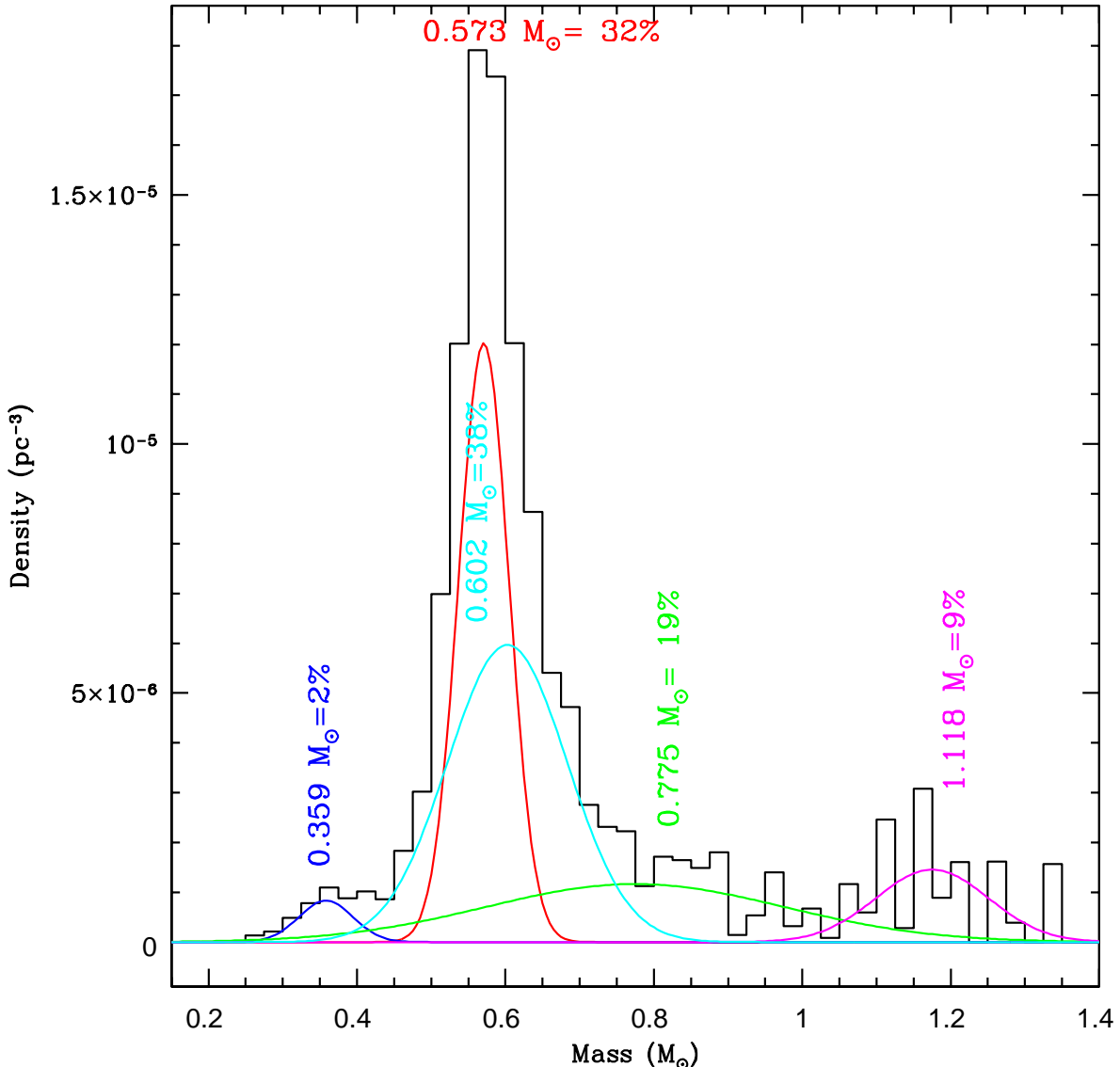
Figures 8 and 9 show the resulting corrected mass distribution for our DA and DB sample, respectively. Figure 8 contains 1733 bright, non-cool DAs, i. e., those with  $T_{\text{eff}} \geq 12\,000$  K and  $g \leq 19$ . We also list the corresponding five Gaussian fit parameters in Table 4. Figure 9 contains 150 bright, non-cool DBs, i. e., those with  $T_{\text{eff}} \geq 16\,000$  K and  $g \leq 19$ . The corresponding three Gaussian fits are listed in Table 5.

Since the most massive white dwarf stars have smaller luminosities because of their smaller radii, after applying the  $1/V_{\text{max}}$  correction to the observed volume, we find that



**Figure 7.** Distribution of distances,  $d$ , and height above the Galactic plane,  $z$ , for DAs in the SDSS DR4.

around 20% DAs are more massive than  $0.8 M_{\odot}$  in our bright and hot sample, of the same order as that discovered by Liebert, Bergeron, & Holberg (2005) for the PG sample. The DB distribution is interesting, however, as it tends to significantly higher masses than does the DA distribution! We found only two stars from our sample with published atmospheric parameters in the literature, with  $\Delta T_{\text{eff}} = 510 \pm 30$  and  $\Delta \log g = 0.12 \pm 0.15$ , so we could not do a comparison as Kleinman et al. (2004) and Eisenstein et al. (2006) did for the DA results.

SDSS DR4 DAs  $g < 19$   $T_{\text{eff}} > 12000\text{K}$ 

**Figure 8.** Histogram for the 1733 DA stars brighter than  $g=19$  and hotter than  $T_{\text{eff}} = 12000$  K corrected by  $1/V_{\text{max}}$ .

## 7 EXTREME MASS STARS

Nalezyty & Madej (2004) published a catalog of all massive white dwarf stars then known, with 112 stars more massive than  $0.8M_{\odot}$ . The four stars with  $\mathcal{M} \geq 1.3M_{\odot}$  in their list are magnetic ones and therefore have large uncertainties in their estimated masses. Dahn et al. (2004) found one non-magnetic massive white dwarf, LHS 4033, with  $\mathcal{M} \simeq 1.318 - 1.335M_{\odot}$ , depending on the core composition. Our oxygen-neon core mass for their derived  $T_{\text{eff}} = 10\,900$  K and  $\log g = 9.46$  is  $\mathcal{M} \simeq 1.30M_{\odot}$ . We note that the models from the Montreal group used to derive  $T_{\text{eff}}$  and  $\log g$  in Dahn et al. (2004) show the same increase in

**Table 4.** Gaussian fits for the  $T_{\text{eff}} \geq 12\,000$  K and  $g \leq 19$  volume corrected DA mass histogram.

i	$a_i$	$M_i(\mathcal{M}_\odot)$	$\sigma_i$	Fraction
1	$5.965 \times 10^{-6}$	0.603	0.081	38%
2	$1.203 \times 10^{-5}$	0.571	0.034	32%
3	$1.165 \times 10^{-6}$	0.775	0.201	19%
4	$1.455 \times 10^{-6}$	1.175	0.076	9%
5	$8.305 \times 10^{-7}$	0.358	0.037	2%

**Table 5.** Gaussian fits for the volume corrected histogram of the 150 DBs brighter than  $g=19$  and hotter than  $T_{\text{eff}} = 16\,000$  K.

i	$a_i$	$M_i(\mathcal{M}_\odot)$	$\sigma_i$	Fraction
1	$8.6 \times 10^{-7}$	0.718	0.111	66%
2	$8.9 \times 10^{-7}$	0.715	0.045	27%
3	$2.9 \times 10^{-7}$	1.286	0.031	7%

mass with decreasing  $T_{\text{eff}}$  as our models and therefore we do not take this mass determination as completely reliable due to the objects relatively low temperature. For GD 50 (WD J0348-0058), Dobbie et al. (2006) found  $T_{\text{eff}} = 41\,550 \pm 720$  K and  $\log g = 9.15 \pm 0.05$ . Our oxygen-neon core mass for their derived  $T_{\text{eff}}$  and  $\log g$  is  $\mathcal{M} \simeq 1.23 \pm 0.02\mathcal{M}_\odot$ , very similar to the value reported by them for C/O models. They also show this massive star is consistent with its formation and evolution as a single star, not the product of a merger.

From the 7167 pure DA white dwarf stars, we found 1611 (22%) with  $\mathcal{M} > 0.8\mathcal{M}_\odot$ . For the 2945 stars brighter than  $g=19$  we found 760 (26%) with  $\mathcal{M} > 0.8\mathcal{M}_\odot$ , but for the 1733 stars brighter than  $g=19$  and hotter than  $T_{\text{eff}} = 12\,000$  K, we find only 105 stars (6%) with  $\mathcal{M} > 0.8\mathcal{M}_\odot$ . The most massive star in our hot and bright sample is SDSS J075916.53+433518.9, whose spectrum spSpec-51883-0436-045 is shown in Fig. 10, with  $g=18.73$ ,  $T_{\text{eff}} = 22\,100 \pm 450$  K,  $\log g = 9.62 \pm 0.07$ ,  $\mathcal{M} = 1.33 \pm 0.01\mathcal{M}_\odot$ , and estimated distance of  $d = 104 \pm 4$  pc. We caution that the evolutionary models used to estimate the radii, and therefore the masses, in our analysis do not include post-newtonian corrections, important for masses above  $\mathcal{M} \simeq 1.30\mathcal{M}_\odot$  (Chandrasekhar & Tooper 1964). For the stars brighter than  $g=19$ , we find 21 others with masses larger than  $\mathcal{M} = 1.3\mathcal{M}_\odot$ , all below  $T_{\text{eff}} = 9\,000$  K. We deem the mass determinations for stars cooler than  $T_{\text{eff}} \simeq 12\,000$  K unreliable. In Table 6, we list the DAs with  $1.2\mathcal{M}_\odot < \mathcal{M} < 1.3\mathcal{M}_\odot$  hotter than  $T_{\text{eff}} = 12\,000$  K.

The spectrum for the brighter  $g=17.99$  SDSS J094655.94+600623.4 is shown in Figure 11. Because our analysis uses relatively low SNR spectra and gravity effects dominate mainly below 3800Å, where we have no data, our conclusion is that we must undertake a study

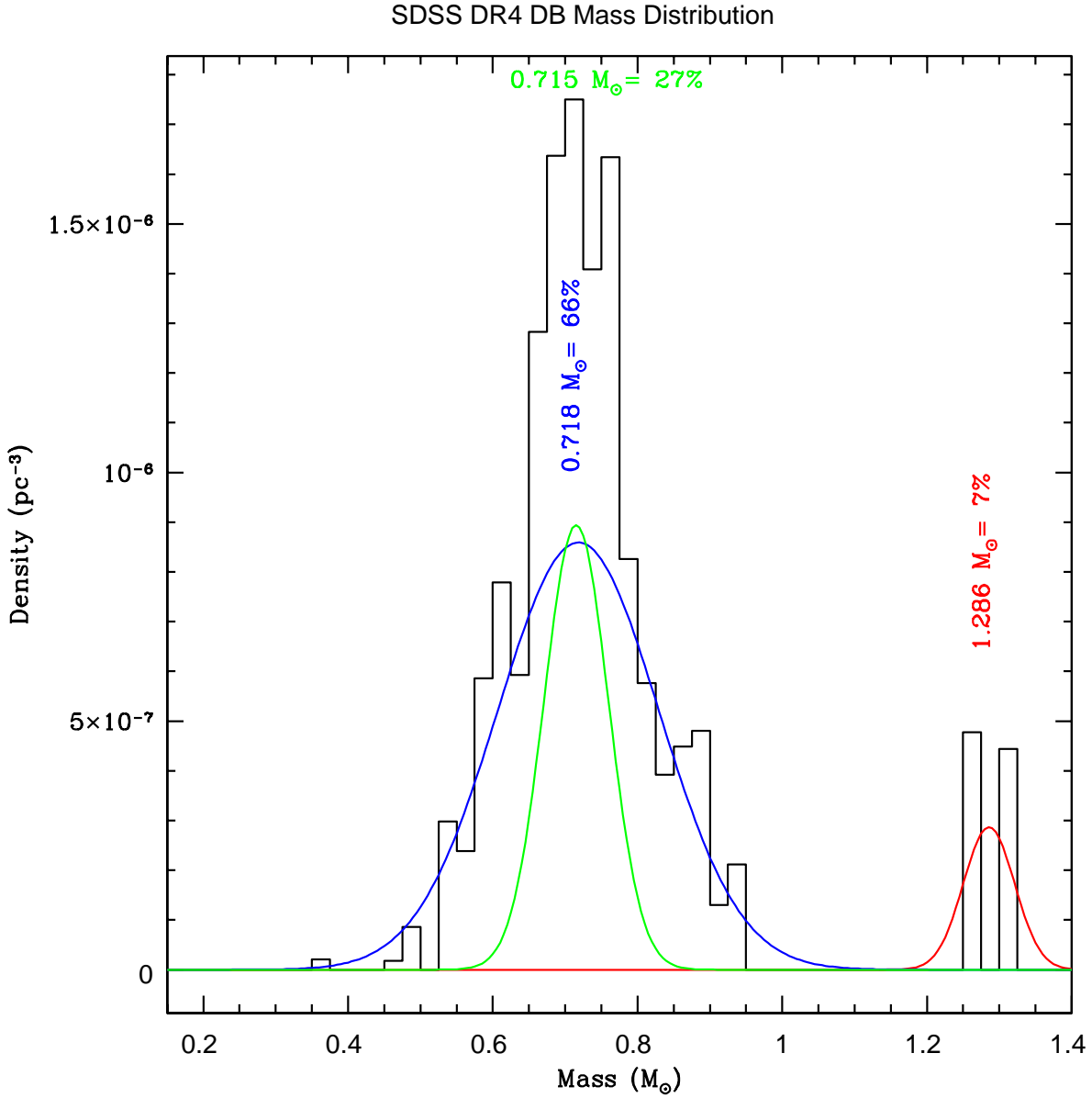


**Figure 9.** Histogram for the 150 DBs brighter than  $g=19$ , and hotter than  $T_{\text{eff}} = 16\,000$  K in DR4, corrected by volume.

Spectra-M-P-F	Name	$g$	$M_g$	$T_{\text{eff}}$ (K)	$\sigma_T$ (K)	$\log g$	$\sigma_g$	$\mathcal{M}$ ( $M_{\odot}$ )	$\sigma_M$ ( $M_{\odot}$ )	$d$ (pc)
spSpec-51691-0342-639	SDSS J155238.21+003910.3	18.44	12.23	15924	387	9.280	0.050	1.262	0.010	97
spSpec-51915-0453-540	SDSS J094655.94+600623.4	17.99	10.87	28125	220	9.370	0.040	1.287	0.010	123
spSpec-52374-0853-198	SDSS J133420.97+041751.1	18.52	12.34	17549	422	9.150	0.060	1.223	0.020	125
spSpec-52703-1165-306	SDSS J150409.88+513729.1	18.84	10.28	79873	8228	9.050	0.390	1.204	0.100	468
spSpec-52751-1221-177	SDSS J110735.32+085924.5	18.42	12.23	18715	327	9.140	0.060	1.219	0.020	128
spSpec-52872-1402-145	SDSS J154305.67+343223.6	18.33	10.85	30472	313	9.300	0.070	1.269	0.010	168

**Table 6.** DA stars with masses above  $1.2 M_{\odot}$  and below  $1.3 M_{\odot}$  derived from the SDSS spectra, with  $T_{\text{eff}} \geq 12\,000$  K.

SDSS J075916.53+433518.9  $g=18.73$   $T_{\text{eff}}=22100\pm450\text{K}$   $M=1.33\pm0.01\text{ M}_{\odot}$

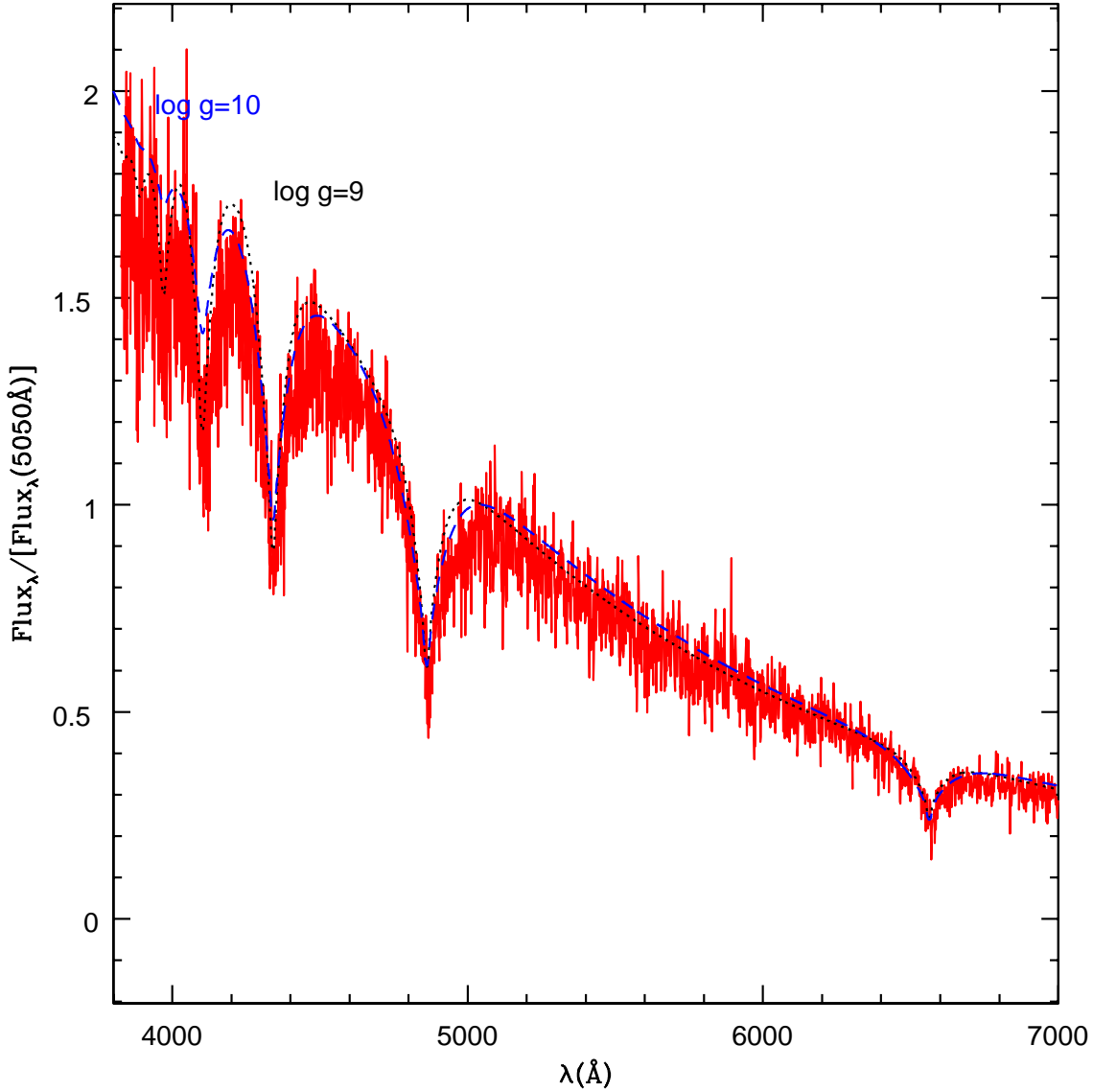


**Figure 10.** Spectrum of SDSS J075916.53+433518.9 with  $g=18.73$ ,  $T_{\text{eff}}=22100\text{ K}$  and two models, with  $\log g=9$  and 10. The higher  $\log g$  fits the H $\alpha$  line better, but the lower  $\log g$  fits the higher lines better, where the SNR is smaller. This low SNR is typical for the stars closer to our upper cutoff of  $g=19$ .

in the violet or ultraviolet to measure the masses more accurately. An extensive study of gravitational redshift would also be critical.

For the 507 single DBs we find 30 DBs with  $\log g > 9$ . Most of our massive DBs are cooler than  $T_{\text{eff}} \simeq 16\,000\text{ K}$ , or fainter than  $g=19$ , except for SDSS J213103.39+105956.1 with  $g=18.80$ ,  $T_{\text{eff}}=16476\pm382$ , and  $\log g=9.64\pm0.21$ , corresponding to a mass  $\mathcal{M}=1.33\pm0.04\mathcal{M}_{\odot}$ , and for SDSS J224027.11-005945.5 with  $g=18.82$ ,  $T_{\text{eff}}=17260\pm402$ , and  $\log g=9.31\pm0.20$ , corresponding to a mass  $\mathcal{M}=1.25\pm0.06\mathcal{M}_{\odot}$ .

The low mass stars present in our sample are consistent with He core evolution models

SDSS J094655.94+600623.4  $g=18$   $T_{\text{eff}}=28100\pm220\text{K}$   $M=1.29\pm0.01$   $M_{\odot}$

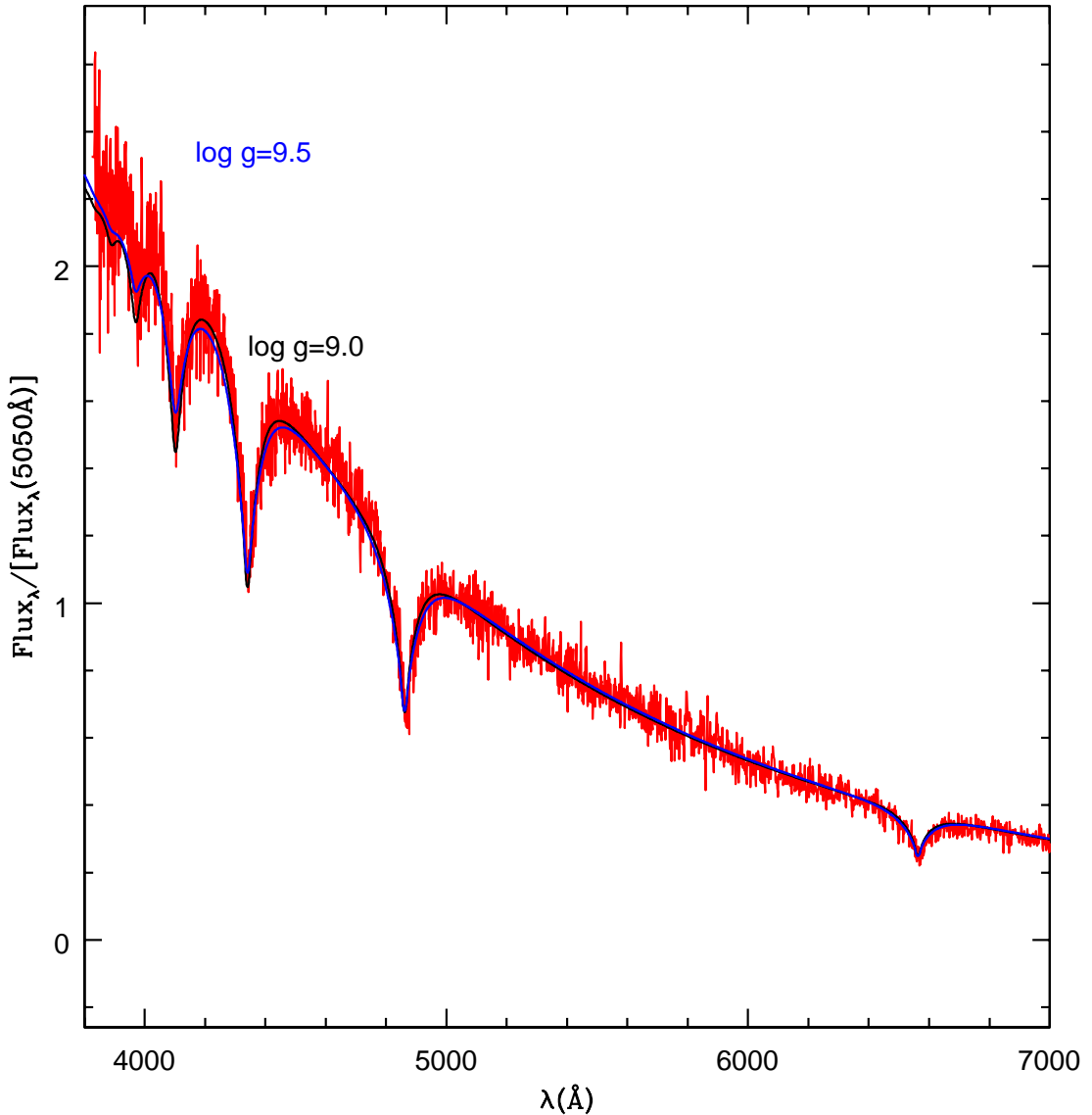


**Figure 11.** Spectrum of SDSS J094655.94+600623.4 with  $g=17.99$ ,  $T_{\text{eff}} = 28100$  K and two models, with  $\log g = 9$  and 9.5. This spectrum is typical of the the SNR achieved for the 1003 DAs and 59 DBs brighter than  $g=18$  in our sample.

calculated by Althaus, Serenelli, & Benvenuto (2001), and displayed in Fig.12. It is important to stress that these stars should be studied with more accurate spectra and model atmospheres, as they are possible progenitors of SN Ia if they accrete mass from companions.

## 8 CONCLUSIONS

Our investigations into the mass distribution of the SDSS DR4 white dwarf sample from Eisenstein et al. (2006) revealed several items. First, all groups are seeing nearly identical

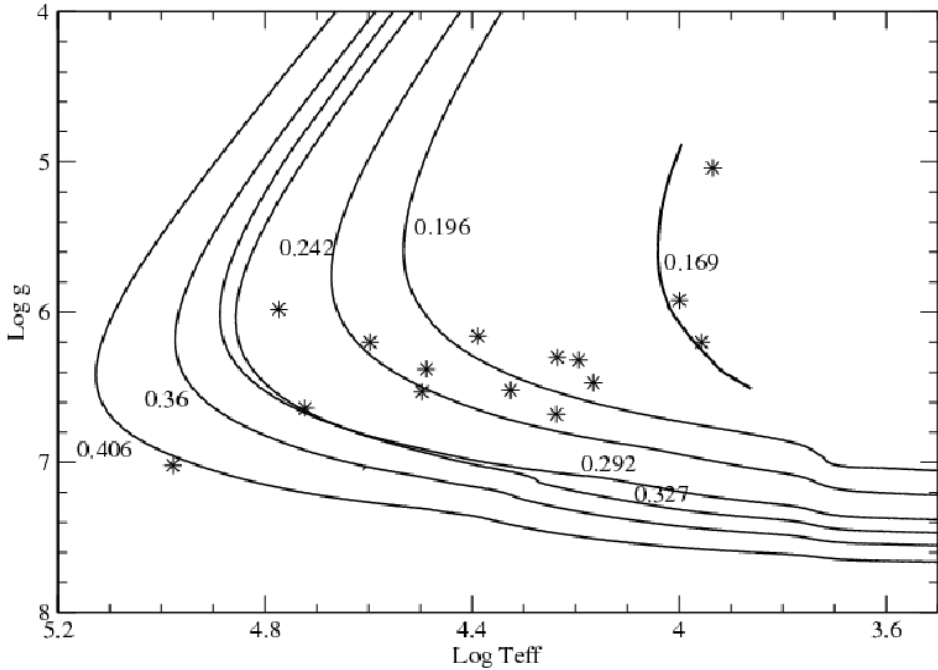


**Figure 12.** Evolutionary tracks for He white dwarf stars calculated by Althaus, Serenelli, & Benvenuto (2001) and the location of the lowest mass stars in our sample. Most of these stars are below  $g=19$  and therefore have noisy spectra.

increases in mean DA at lower temperatures (less than  $\approx 12\,000\text{K}$  for DAs and  $16\,000\text{K}$  for DBs). Either this is truly going on in the white dwarf stars, or there is missing or incorrect physics in everyone's models. We propose the treatment of neutral particles as the most likely explanation. We suspect the atmospheric models should be improved with a detailed inclusion of the line broadening by neutral particles, since the increase in apparent mass for both DAs and DBs occur at temperatures when recombination becomes important.

Secondly, we find a significant difference between the DA and DB mass distributions, with the DB distribution significantly more weighted to massive stars. Figs. 13 and 14 show the combined number and volume-corrected DA and DB histograms. The DB histograms have been re-normalized to the DA maximum for display purposes. Our results contradict nearly all previous work which show the mean DA and DB masses to be similar (with the exception of Koester et al. 2001). We note that the previous efforts, though, were based on histograms for DBs with less than 50 stars, and our DB histogram has 150 stars. However, we still need to explore our DB models and fits in more detail to verify the validity of this novel result. Specifically, we find  $\langle M \rangle_{\text{DB}} = 0.711 \pm 0.009 M_{\odot}$ , higher than  $\langle M \rangle_{\text{DA}} = 0.593 \pm 0.016 M_{\odot}$ .

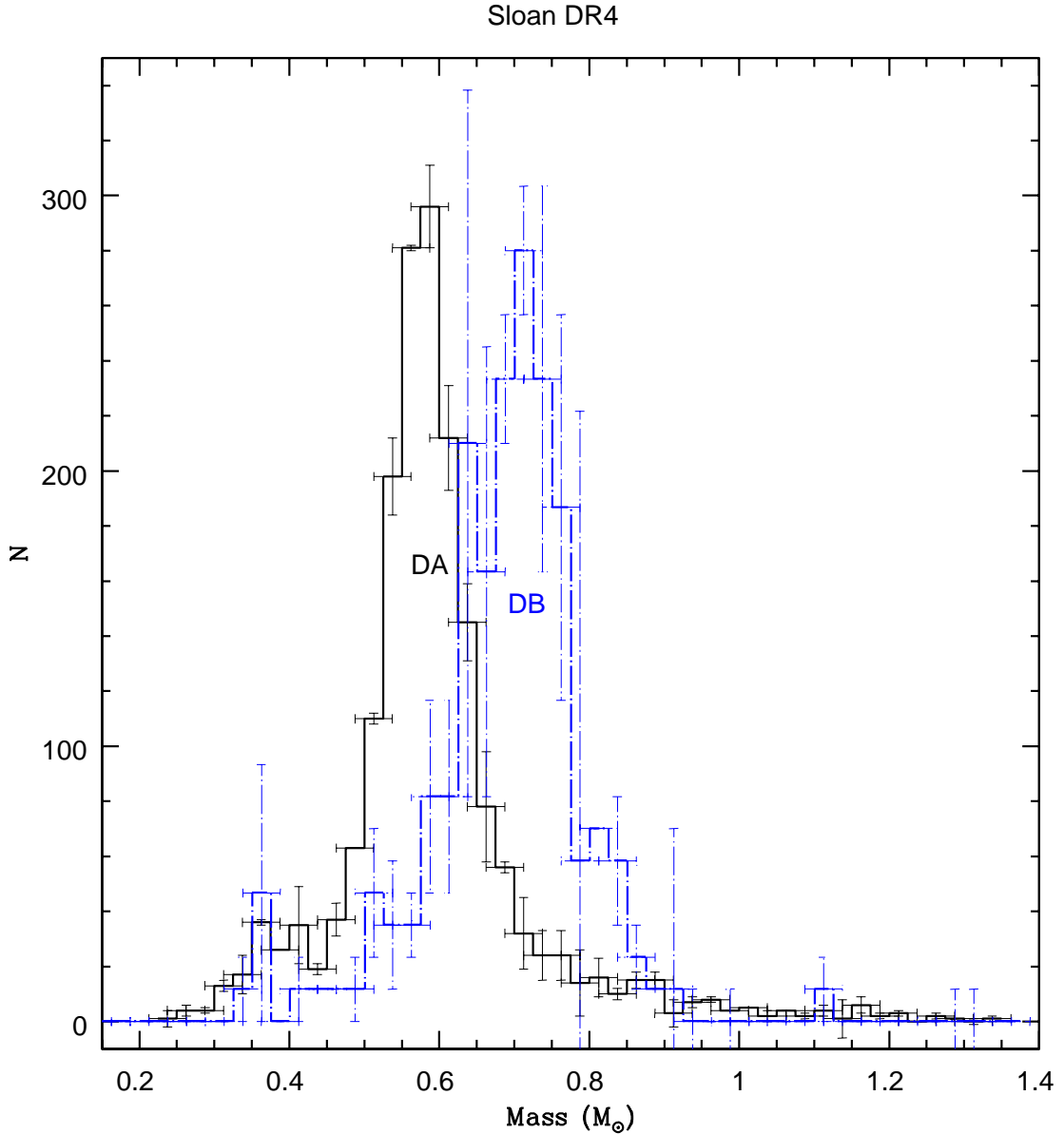


**Figure 13.** DA and DB histograms for comparison. The DB histogram has been re-normalized to the DA maximum for display purposes.

for the 1733 DAs brighter than  $g=19$ , and hotter than  $T_{\text{eff}} = 12000$  K. This is a significant new result and must be investigated further.

We have also detected a large number of massive DA white dwarf stars: 760 with  $\mathcal{M} > 0.8\mathcal{M}_\odot$  brighter than  $g=19$  and 105 both brighter than  $g=19$  and hotter than  $T_{\text{eff}} = 12000$  K. We report the highest  $\log g$  white dwarf ever detected.

## ACKNOWLEDGMENTS

We thank Dr. Daniel Eisenstein for some helpful suggestions, and his *autofit* code, and the referee, Dr. Martin Barstow, for very detailed and useful comments that improved the presentation of the paper.

## REFERENCES

Althaus L. G., Serenelli A. M., Benvenuto O. G., 2001, MNRAS, 323, 471

Althaus L. G., García-Berro E., Isern J., Córscico A. H., 2005, A&A, 441, 689

Arras P., Townsley D. M., Bildsten L., 2006, ApJ, 643, L119

Beauchamp A., 1995, Ph. D. Thesis, Université de Montreal.

Bergeron P., Saffer R. A., Liebert J., 1991, White Dwarfs, NATO ASI Series 336, eds. G. Vauclair and E. Sion, 75

Bergeron P., Wesemael F., Fontaine G., 1991, ApJ, 367, 253

Bergeron, P., Wesemael, F., Lamontagne, R., Fontaine, G., Saffer, R. A., & Allard, N. F. 1995, ApJ, 449, 258

Bohm, K. H., & Cassinelli, J. 1971, A&A, 12, 21

Bradley P. A., 2006, MmSAI, 77, 437

Bradley P. A., 2001, ApJ, 552, 326

Bradley P. A., 1998, ApJS, 116, 307

Castanheira B. G., Kepler S. O., Handler G., Koester D., 2006, A&A, 450, 331

Chandrasekhar S., Tooper R. F., 1964, ApJ, 139, 1396

Dahn C. C., Bergeron P., Liebert J., Harris H. C., Canzian B., Leggett S. K., Boudreault S., 2004, ApJ, 605, 400

Dobbie P. D., Napiwotzki R., Lodieu N., Burleigh M. R., Barstow M. A., Jameson R. F., 2006, MNRAS, 373, L45.

Eisenstein, D. J., et al. 2006, ApJSS, 167, 40.

Finley D. S., Koester D., Basri G., 1997, ApJ, 488, 375

Fleming T. A., Liebert J., Green R. F., 1986, ApJ, 308, 176

Fontaine G., Wesemael F., 1991, IAUS, 145, 421

Fontaine G., Wesemael F., 1997, White, dwarfs, Proc. 10th European Workshop on White Dwarfs, eds. Isern, J.; Hernanz, M.; Garcia-Berro, E., (Dordrecht: Kluwer), ASSL Series, 214, 173

Geijo E. M., Torres S., Isern J., García-Berro E., 2006, MNRAS, 369, 1654

Green R. F., 1980, ApJ, 238, 685

Harris H. C., et al., 2006, AJ, 131, 571

Herwig F., 2004, ApJS, 155, 651

Kepler, S. O., Castanheira, B.G., Costa, A.F.M., & Koester, D. 2006, MNRAS, 372, 1799.

Kepler S. O., Castanheira B. G., Saraiva M. F. O., Nitta A., Kleinman S. J., Mullally F., Winget D. E., Eisenstein D. J., 2005, A&A, 442, 629

Kleinman, S. J., et al. 2004, ApJ, 607, 426

Koester D., 1991, in Proc. 7th European Workshop on White Dwarfs, NATO ASI Ser., ed. G. Vauclair & E. M. Sion (Dordrecht: Kluwer), 343

Koester D., et al., 2001, A&A, 378, 556

Engelbrecht, A. & Koester, D. 2007, in 15th European White Dwarf Workshop, eds. R. Napiwotzki & M. Barstow, APS, in press.

Lawlor T. M., MacDonald J., 2006, MNRAS, 371, 263.

Lemke M., 1997, A&AS, 122, 285

Liebert J., Bergeron P., Holberg J. B., 2005, ApJS, 156, 47

Madej J., Nalezyty M., Althaus L. G., 2004, A&A, 419, L5

Marsh M. C., et al., 1997, MNRAS, 286, 369

McCook, G. P., & Sion, E. M. 2003, VizieR Online Data Catalog, 3235, 1

Metcalfe T. S., 2005, MNRAS, 363, L86

Metcalfe T. S., Nather R. E., Watson T. K., Kim S.-L., Park B.-G., Handler G., 2005, A&A, 435, 649

Moehler S., Koester D., Zoccali M., Ferraro F. R., Heber U., Napiwotzki R., Renzini A., 2004, A&A, 420, 515

Nalezyty M., Madej J., 2004, A&A, 420, 507

Napiwotzki R., Green P. J., Saffer R. A., 1999, ApJ, 517, 399

Oke J. B., Weidemann V., Koester D., 1984, ApJ, 281, 276

Richer, H. B., et al. 2007, in 15th European White Dwarf Workshop, eds. R. Napiwotzki & M. Barstow, APS, in press.

Schmidt M., 1968, ApJ, 151, 393

Vennes S., 1999, ApJ, 525, 995

Vennes S., Thejll P. A., Galvan R. G., Dupuis J., 1997, ApJ, 480, 714

Vennes S., et al., 2005, in White Dwarfs as Cosmological and Galactic Probes, eds. H.L.

Shipman, E.M. Sion and S. Vennes (Dordrecht: Kluwer), 49  
York D. G., et al., 2000, AJ, 120, 1579  
Wilson, L. A., 2000, ARA&A, 38, 573  
Wood, M. A. 1995, in Koester, D. & Werner, K., eds., LNP Vol. 443: White Dwarfs,  
Springer-Verlag, Berlin, p. 41

This paper has been typeset from a  $\text{\TeX}$ /  $\text{\LaTeX}$  file prepared by the author.

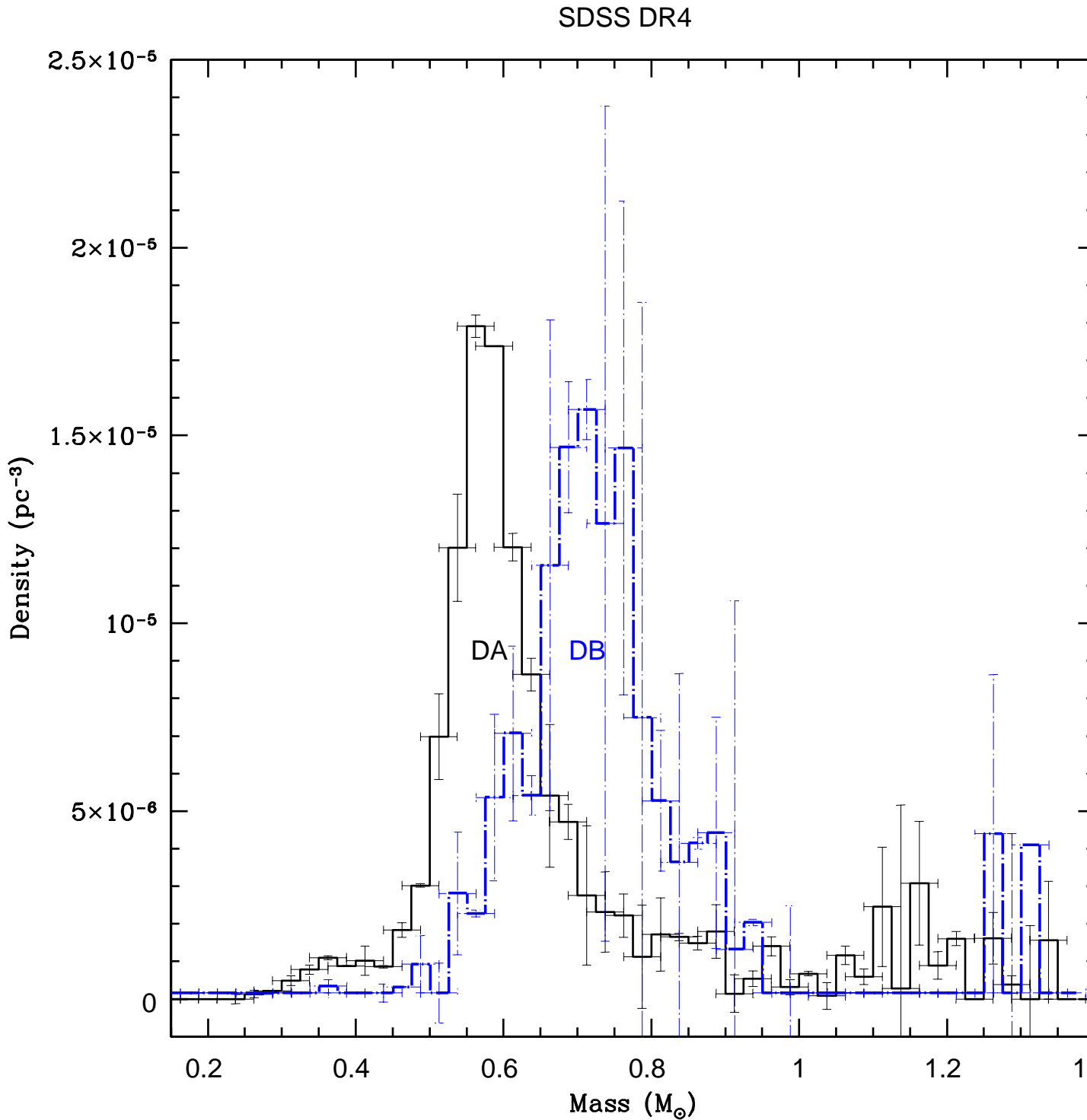


**Figure 14.** DA and DB histograms corrected by observed volume for comparison. The DB histogram has been re-normalized to the DA maximum for display.